Indonesian Geotechnical Journal, August 2024, Vol 3 (2). Page 1-16
DOI: https://doi.org/10.56144/igj.v3i1.79
EISSN: 2829-7520
https://indonesian-geotechnical-journal.org/index.php/JGI/issue/archive

Fiber-Reinforcement MICP for Durability Improvements

Lutfian R Daryono[1,*], Tomohiko Abe[1], Masanao Kano[2], Kazunori Nakashima[3], Satoru Kawasaki[3]

[1]Engineering and Development Divisions, NITTOC Construction Co., Ltd., Japan
[2]Division of Sustainable Resources Engineering, Graduate School of Engineering, Hokkaido University, Japan
[3]Division of Sustainable Resources Engineering, Faculty of Engineering, Hokkaido University, Japan

*Correspondence: luthfian.daryono@gmail.com; lutfian.rusdi.daryono@nittoc.co.jp

SUBMITTED 29 October 2023 **REVISED** 18 March 2024 **ACCEPTED** 25 August 2024

ABSTRACT Microbially Induced Carbonate Precipitation (MICP) technology, a method for soil enhancement, has recently garnered considerable attention within geotechnical communities. This study places a significant focus on addressing the paramount concern pertaining to the endurance of MICP-treated specimens. The research centers on MICP-treated samples fortified with plant-derived natural fibers, specifically jute, and evaluates their robustness when subjected to exposure to both distilled water (DW) and artificial seawater (ASW). The primary objectives encompass acquiring a comprehensive understanding of their prolonged performance under varied conditions, appraising the effects of fiber reinforcement, and augmenting the suitability of MICP-treated samples for applications in safeguarding coastal regions against erosion. The investigation subjected these specimens to 12 wetting-drying cycles utilizing artificial seawater and distilled water following treatment periods of 5 days, 7 days, and 14 days. The findings unveiled an approximate 8.5% diminution in sample mass, with the fibers constituting 2% of the sand's total weight based on WD cycle tested. The UCS needle penetration test confirmation tests were done with one of the samples ruptured and one of the samples decreased 30% in strength due to the WD cycled. Moreover, the study underscores the adeptness of the integrated fiber in withstanding the wetting-drying (WD) cyclic process, amplifying the mechanical and physical attributes of the fiber-reinforced MICP-treated specimens, thus contributing significantly to their overall durability about 17% from the results, respectively.

KEYWORDS Erosion; MICP; Durability; Fiber-Reinforcement; Bio-Cement

1 INTRODUCTION

A notable and environmentally friendly methodology that has garnered significant scholarly attention in recent times is Microbial-Induced Carbonate Precipitation (MICP). This innovative technique leverages biological processes for the creation of calcium carbonate bio-cement, relying on the enzymatic activity of microbial urease. This critical aspect has been thoroughly discussed in research conducted by DeJong et al. (2010) and Portugal et al. (2020). The significance of MICP extends beyond its ecological implications, as it offers promising applications in various fields including geotechnical engineering and environmental remediation.

Among the various pathways for Microbial-Induced Carbonate Precipitation, the ureolytic process stands out as a subject worthy of comprehensive exploration. This process unfolds straightforwardly, commencing with the conversion of urea ($CO(NH_2)_2$) into ammonia (NH_3) and carbonic acid (H_2CO_3) through a sequence of reactions (as outlined in Equations 1-4), as elucidated by Burne and Chen (2000). Subsequently, ammonia and carbonic acid reach equilibrium in an aqueous medium, resulting in the generation of bicarbonate (HCO_3^-), ammonium (NH_4^+), and a hydroxide ion (OH^-) (as explained in Equations 5 and 6). It is at this juncture that a crucial increase in pH occurs, a prerequisite condition for calcite precipitation. This pH elevation in turn, prompts the bicarbonate equilibrium to shift towards the formation of carbonate ions (CO_3^{2-}), as per Equation 6. These ions precipitate as calcium carbonate ($CaCO_3$) when there is an excess of soluble calcium (Ca^{2+}), as

expounded by Burne and Chen (2000) and Castanier et al. (1999). A high carbonate concentration leads to the precipitation of $CaCO_3$ around the cells, driven by the presence of calcium ions in the surrounding environment as described in Equation 9.

In natural settings, carbonate precipitation occurs at a leisurely pace. In this context microorganisms act as catalysts, hastening the carbonate formation process. Carbonates, particularly calcite ($CaCO_3$) and dolomite ($CaMg(CO_3)_2$), form the composition of surface limestones and represent a significant reservoir of carbon within the lithosphere, as highlighted by Ehrlich and Newman (2009) and Kumari et al. (2016). However, despite our growing understanding of this intricate process, the mechanisms governing biological carbonate precipitation remain only partially elucidated. The experience with and optimization of the ureolytic process are pivotal for harnessing the full potential of MICP in these domains. Exploring the interactions between microbial activity, geochemical processes, and the geotechnical implication of MICP promises a multifaceted and holistic approach to the subject matter, one that bridges ecological, geological, and engineering perspectives.

$$CO(NH_2)_2 + H_2O \rightarrow NH_2COOH + NH_3 \quad (1)$$

$$NH_2COOH + H_2O \rightarrow NH_3 + H_2CO_3 \quad (2)$$

$$CO(NH_2)_2 + 2H_2O \rightarrow 2NH_3 + H_2CO_3 \quad (3)$$

$$H_2CO_3 \leftrightarrow HCO_3^- + H^+ \quad (4)$$

$$2NH_3 + 2H_2O \leftrightarrow 2NH_4^+ + 2OH^- \quad (5)$$

$$2HCO_3^- + 2H^+ + 2OH^- + 2NH_3 \leftrightarrow 2CO_3^{2-} + 2NH_4^+ + 2H_2O \quad (6)$$

$$Ca^{2+} + cell \leftrightarrow cell : Ca^{2+} \quad (7)$$

$$CO_3^{2-} + cell : Ca^{2+} \leftrightarrow cell: CaCO_3 \quad (8)$$

$$CO(NH_2)_2 + 2H_2O + Ca^{2+} \leftrightarrow 2NH_4^+ + CaCO_3 \quad (9)$$

The primary aim of this investigation is to explore the potential of bio-cement treatment with sand material and assess their durability, especially under saturated conditions. The findings revealed that MICP-treated specimens subjected to prolonged wetting-drying tests, simulating extended exposure, exhibited an average mass loss ranging from 3% to 9% at the culmination of 12 cycles, as documented by Gowthaman (2022).

This research accelerated the time period of solidification by calcium ions with added fiber content to assess their durability.

Moreover, it has become apparent that the degree of cementation significantly influences the rate of mass loss. Based on this results are approximately 8.5% diminution in sample mass, with the fibers constituting 2% of the sand's total weight based on WD cycle tested. The UCS needle penetration test confirmation tests were done with one of the samples ruptured and one of the samples decreased 30% in strength due to the WD cycled with the comparison around 17% effectiveness by added fibers in the MICP processes. This observation suggests a vital link between the level of cementation and the specimens' response to wetting-drying cycles, shedding light on the intricacies of their behavior. The mechanism behind this short-term degradation can be clarified by examining the progression of calcium carbonate precipitates during the MICP treatment process. Initially, calcium carbonates appear as irregular, non-crystalline deposits. However, over time, these deposits mature and undergo a transformation into well-defined calcium carbonate crystals, such as calcites, within the aqueous environment. This evolution of calcium carbonate structures, as elucidated by Daryono (2020a), offers valuable insights into the dynamic processes that operate during MICP treatment. To closely simulate the real-life situation, the concentration of DW and ASW were maintained by using fresh distilled water or artificial seawater every cycle.

Addressing the limitation, as mentioned earlier, has prompted numerous studies aimed at enhancing the ductility and toughness of sand following MICP curing (Muthukkumaran, et al., 2016; Liu, et al., 2019; Imran, et al., 2022). The integration of fibrous materials stands out as a promising avenue for enhancing these attributes. This approach opens new horizons for fortifying the structural and mechanical aspects of MICP-treated soil. Earlier studies have mainly centered around fibers derived from synthetic polymers, such as non-woven geotextiles, steel, polypropylene, glass, and carbon fibers were mainly focus on Portland cement reinforcement (Kujawa, et al., 2021; Soupionis, et al., 2020). However, these materials come with concerns related to environmental impacts by using PVA, as underscored by Choi et al. (2016) and Gowthaman et al. (2018). As a result, the long-term performance of MICP-treated sand continues to be a topic of interest in the domain. Few experiments have delved into enhancing the engineering properties of MICP-treated soils using fiber materials, as detailed in Table 1. As the world moves towards more sustainable construction practices, it is imperative to conduct more extensive research to formulate advanced engineering solutions. In demand are affordable, accessible fibers that align with performance metrics, global sustainability, safety, and environmental goals.

Table 1. Biochemical compositions and the physical-mechanical properties of plant fibers in reinforcing the soil (modified after Gowthaman, et al., 2018)

Source of Fiber	Fiber Origin	Cellulose (%)	Hemicellulose (%)	Lignin (%)	Density (kg/m^3)	Young's Modulus (GPa)	Ultimate Tensile Strength (MPa)	Moisture Absorption (%)
Bamboo	Culm	40-55	18-20.8	15-32.2	715-1225	33-40	400-1000	40-53
Jute	Stem	56-71	29-35	11-14	1300-1450	10-30	393-860	12
Coir	Fruit	32-43	21	40-45	1390-1520	3-6	100-225	130-180
Palm	Fruit	32-35.8	24.1-28.1	26.5-28.9	463	26-32	100-400	1-10
Sugarcane Bagasse	Stem	32-44	25	19-24	1250	15-19	66.3-290	-
Water Hyacinth	Stem	43.5-47.3	19.8-22.3	5.5-13.1	800	-	295.5-329.5	32
Rice	Husk	59.9	59.9	20.6	-	-	-	-
Sisal	Leaf	57-71	16	11-12	700-1330	9-20	400-700	56-230
Flax	Stem	62-72	18.6-20.6	2-5	1500	27.6-80	345-1500	7
Banana	Leaf	60-65	25	5-10	1350	27-32	711-779	-
Hemp	Stem	67-78.3	5.5-16.2	2.9-3.7	1140-1470	30-70	690-920	8-9
Kenaf	Stem	70	3	19	1040	136	1000	307
Pine	Straw	67.3	67.3	11.6	813	-	61.65	-
Barely	Straw	33-40	20-35	8-17	870	-	-	400
Wheat	Straw	30	50	15	868	-	-	280-350

The comprehensive analysis in this paper seeks to rectify the inherent shortcomings present in the conventional MICP methodology by examining the potential benefits of integrating fibers into MICP-treated sand. The research delved into samples of MICP-treated sand reinforced with jute-based natural fibers, assessing their endurance when exposed to distilled water (DW) and simulated seawater (ASW). This study provides a valuable understanding of their long-standing performance metrics and the impact of fiber fortification. A further objective of this study is to enhance the applicability of MICP-treated specimens in resisting coastal degradation.

2 METHODOLOGY

A sequence of laboratory experiments was undertaken to investigate the parameters that were influenced during the solidification of samples incorporating fiber reinforcement. The solidification process was executed through the syringe solidification method. Subsequently, a needle penetration test was conducted to ascertain the estimated Unconfined Compressive Strength (UCS) value (the standard explained in *the Supplement Material A*).

2.1 MICP Treatment

In our experiment, the Japanese Miyazaki sand was used. Figure 1 provides the particle size distribution of the local beach sand. The specimen was prepared using a 50 ml expendable syringe

barrel, with a 30 mm diameter as mold. Each sample consisted of 60 g of Japanese Miyazaki sand samples of the same density. The sand samples were collected from Miyazaki Shore which consisted of silica-sand with A sample is fresh near the bay and B sample is sedimentary sand are classified old-sedimentary refers to previous publications by Daryono, et al., 2024. After the sand samples were sterilized and dried for 24 hours, then placed in a 30 mL syringes into 6-7 centimeters, respectively. Moreover, 20 mL of a culture medium solution (ZoBell2216E solution) and 20 mL of the cementation media for consolidation were injected into the syringe and drained off leaving about 2 mL of solution above the top surface of the sand. This solution for consolidation was then injected and drained once a day or once every two days and the curing period was 5 days, 7 days, and 14 days.

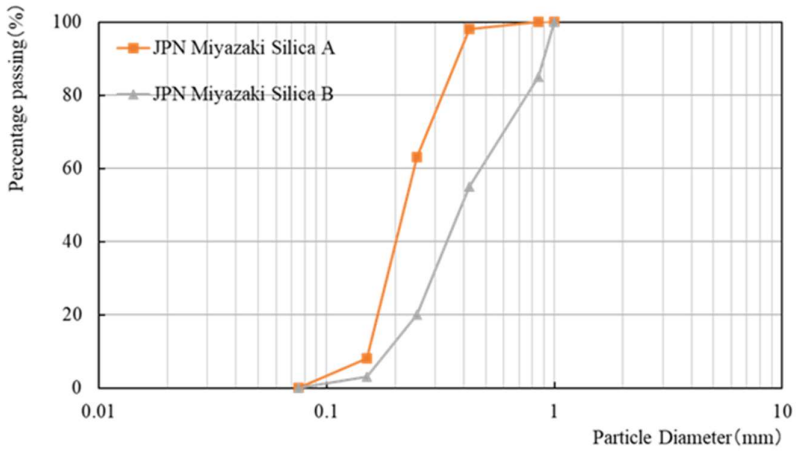

Figure 1. Particle size distribution of local beach sand from Miyazaki Bay, Japan.

To safeguard the integrity of the sample, a filter paper was placed at the base of the syringe barrel before filling. This was to minimize potential sand movement during the treatment phase. Additionally, the incorporation of an extra syringe filter (0.45 μ m) was a calculated decision to curtail the potential detrimental impacts of sizable organic particles in the nutrient medium. Such particles, often overlooked, can critically risk carbonate crystallization, thereby affecting the study's outcomes. The MICP treatment was conducted in two phases following previous research of Gowthaman et al. (2020) and Daryono et al., (2020b). The first phase (day 1) involved a 12 ml introduction of a bacterial culture medium (OD_{600} ranging between 1.5 and 2), setting the stage for the microbial action. OD_{600} is an abbreviation of optical density and 600 nm wavelength used to measure a spectrophotometer method that is used to help estimate the concentration or number of cells per volume of bacteria or other cells within a liquid sample. The second phase was the application of 12 ml cementation solution contained of Ca2+ ions that were reapplied every 24 hours for a total of 7 days. This method optimized the chances of achieving the desired solidification and bonding among sand particles.

2.2 Solution Used for Wetting-Drying Cycle Test

For the wetting-drying cycle testing, two types of solutions were employed: distilled water (DW) and artificial seawater (ASW). Distilled water was chosen to simulate the permeation of rainwater through a beach nourishment embankment, while artificial seawater was utilized to mimic exposure to seawater. The chemical composition of the ASW is tabulated in Table 2.

Table 2. Chemical composition of artificial sea water (ASW) per liter

Compound	g/L
$MgCl_2 \cdot 6H_2O$	11.11
$CaCl_2 \cdot 2H_2O$	1.54
$SrCl_2 \cdot 6H_2O$	0.04
KCl	0.69
$NaHCO_3$	0.2
KBr	0.1
H_3BO_3	0.03
NaF	0.003
NaCl	24.53
Na_2SO_4	4.09

2.3 Jute Fiber Properties

Jute stands out as a predominant natural fiber crop cultivated on a global scale. Aside from its high availability, its economic viability enhances its appeal (Fagone et al., 2017; Akil et al., 2009). Predominantly grown in Asian regions with stature heights ranging between 2.5 to 4.5 meters, jute also finds its presence in Brazil (Summerscales et al., 2010). The remarkable attribute of jute lies in its capability to augment the geotechnical characteristics of soil. Consequently, its integration finds paramount importance in a myriad of applications such as infrastructure construction, bank protection along river courses, stabilization of embankments, erosion control, slope management, and other associated geotechnical operations (Ghosha et al., 2017).

While the significance of jute fibers in geotechnical applications is irrefutable, it is noteworthy that only a niche segment of researchers has delved into unlocking the potential of jute textiles in the realms of drainage and preload applications. Their findings highlight jute textiles as a cost-efficient and dependable strategy, especially in soft soil matrices (Tan et al., 1994; Chattopadhyay and Chakravarty, 2009). The distinctive features of open-weave jute textiles, such as encompassing the triad of flow velocity regulation, optimal moisture absorption, and commendable transparency, further accentuate their value proposition (Ghosha et al., 2017; Ranganathan, 1994). A deeper structural analysis reveals that jute textiles are comprised of an intricate blend of 40% direct yarn coverage juxtaposed with a 60% open expanse. This strategic composition curtails groundwater flow velocities, subsequently minimizing soil erosion and transportation phenomena (Ranganathan, 1994).

In the realm of geotextiles, jute's prominence cannot be understated. Jute geotextiles mitigate soil or sand depletion by acting as a critical intermediary in soil conservation. The efficacy of jute-paved surfaces is evident in their minimal soil loss, even when faced with significantly increased water content, reaching up to 200% (Tan et al., 1994). An intriguing finding is the enhanced tensile strength exhibited by glued/punched jute fabric, which outperforms traditional jute textiles by approximately 30%, highlighting its robustness and suitability for diverse applications (Fagone et al., 2017).

Several significant findings pertaining to jute geotextiles have come to light. Firstly, it has been observed that treated jute geotextiles experience a substantial reduction in tensile strength of approximately 50% over a duration of 1,080 days, as noted in research by Saha et al. (2012).

Secondly, an examination of the strength characteristics of randomly distributed jute fibers within clayey soil has revealed valuable insights. Researchers have explored different fiber dosages ranging from 0.2% to 1% and varied fiber lengths spanning 5 to 20 mm as reported by Al-Swaidani et al. (2016); Gosavi et al. (2004) and Bundela et al. (2015).

Thirdly, it is worth noting that the random distribution of jute fibers plays a pivotal role in mitigating post-peak strength loss in expansive soils by augmenting critical strength parameters and influencing stress-strain behavior (Wang et al., 2017; Kachi et al., 2015; Michalowski and Cermak, 2002; Diambra et al., 2010).

2.4 Test Programme

The cyclic wetting-drying tests comprised of nine distinct tests, as detailed in Table 3. These tests were determined based on the presence of jute fibers (J) or absence of jute fibers (NJ) and the type of soaking solution utilized, i.e., AWS and DW. The treatment periods were selected to align with prior MICP research results (insert reference here), with treatment durations of 5 days or 7 days. However, it should be noted that previous study of jute fiber reinforced MICP sand by Imran et al. (2020) had a treatment period of 14 days. In addition, Imran et al. (2020) experiments used two cycles of bacterial solution (day 0 and day 7). For comparative purposes, one additional test with 14 days period (NJ-14-DW) was added to ascertain whether deterioration due to wetting-drying cycles was observed on sample with longer treatment duration, but the bacterial solution was only applied on day 0.

Table 3. Wetting-drying test cases conditions

Test ID	Fibers	Treatment period	WD condition test
J-5-AWS	YES	5 days	Artificial Seawater
J-7-AWS		7 days	
J-5-DW	YES	5 days	Distilled Water
J-7-DW		7 days	
NJ-5-AWS	NO	5 days	Artificial Seawater
NJ-7-AWS		7 days	
NJ-5-DW	NO	5 days	Distilled Water
NJ-7-DW		7 days	
NJ-14-DW		14 days	

The jute fibers were acquired by unraveling hemp cords made by Hayase Kogyo Co., Ltd. and had a diameter of approximately 0.1 mm. In accordance with prior research conducted by Imran et al. (2020), the quantity of jute fiber is 1.5% to 3%, with the optimum is 3% of the initial sand weight. In this research slightly less ratio was used, the ratio was set at 2% of the mass of Miyazaki Sea sand, equivalent to 1.2 g of jute fiber per specimen. The length of jute fibers used were cut to a fixed length of 15 mm. The mixing procedure is visually represented in Figure 2.

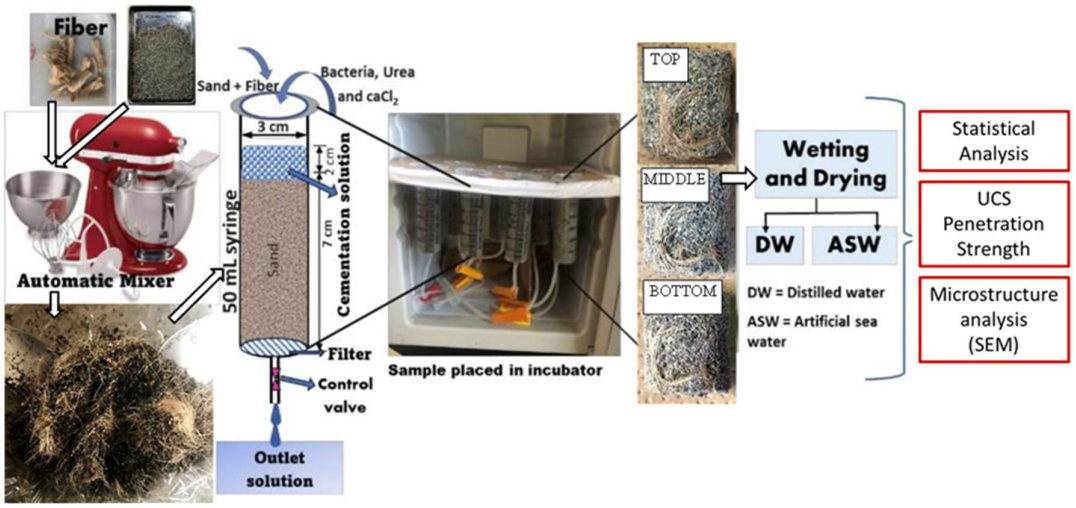

Figure 2. Sample preparation and test setup for the MICP process with the addition of jute fibers (Modified from Imran et al., 2020).

2.5 Evaluation Methods

2.5.1 Effect of Wetting-Drying (WD) Cycles on the Durability

To assess the impact of wetting-drying (WD) cycles on the durability of the specimens, a standardized procedure following ASTM guidelines (2003) was employed. In each WD cycle, the specimens underwent a series of meticulously controlled steps. Initially, they were immersed in room-temperature water (20 ±1° C) for a duration of 6 hours which modified from the ASTM D559-03 from the limitations of equipment. Subsequently, they underwent a thorough drying process, with specimens being placed in an oven set at a minimum temperature of 60±1° C for a minimum duration of 42 hours. This cycle was repeated for a total of 12 cycles. Refer to Figure 4 for a visual representation.

At the end of each WD cycle, the dry mass of the specimen was measured. This assessment was ideally conducted until the mass became constant during the drying process; due to the limitation of the study this research was represented until 12 cycled. Recording of the loss in mass at this stage provided valuable insights into the effects of the wetting-drying test cycles on the specimens.

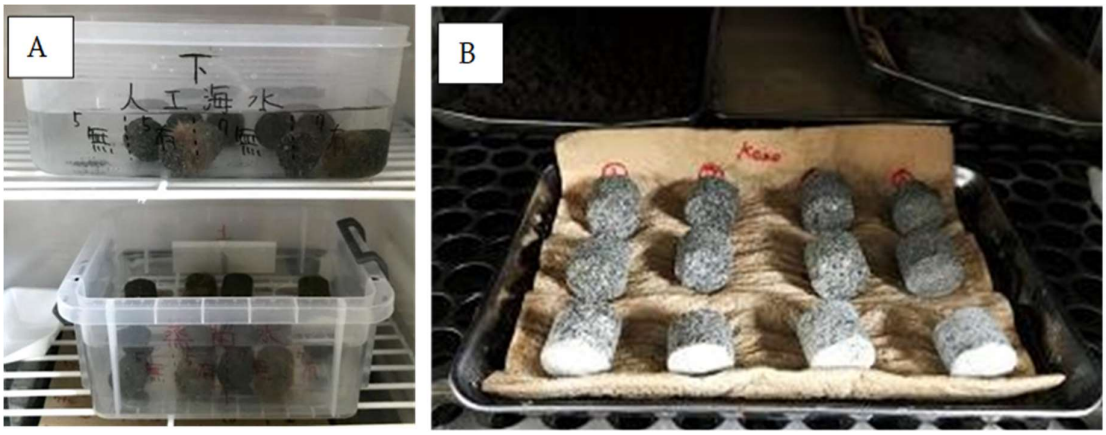

Figure 4. (A) Specimens immersed in water at 20℃ and (B) test specimens placed in constant temperature drying oven at 60℃.

2.5.2 Unconfined Compression Test

The evaluation of cementation strength in the specimens was conducted using a needle penetration (NP) device, specifically the SH-70 soft rock penetrometer from the Maruto Testing Machine Company in Tokyo, Japan. Subsequently, the UCS of the specimens was estimated based on the Np value in accordance with the JGS 3431-2012 standard, as described by Ulusay et al. (2015). This approach underscores the importance of standardized testing procedures, ensuring that the measured properties can be reliably compared across different studies and settings.

The needle penetration apparatus, initially developed in Japan, serves as a portable testing device specifically designed to predict the UCS of materials ranging from soft to fragile rocks and cemented soil specimens. During the testing procedure, the models were oriented horizontally. The device's needle was then utilized to penetrate the cylindrical surface of the sample at three distinct locations: 1 cm from the top, 3 cm from the middle, and 5 cm from the bottom of the column. Importantly, this process enables simultaneous measurement of both penetration load (N) and penetration depth (mm) at each specified locations.

This methodology, utilizing the SH-70 penetrometer in adherence to the JGS 3431-2012 standard, provides a reliable approach in estimating the specimens' UCS. This, in turn, contributes to a comprehensive assessment of their cementation strength and mechanical properties.

The schematic diagram of the NP device is shown in Figure 3. The NP device is composed of eight components, each plays a crucial role in the precise determination of cementation strength. The

procedure entails a gradual withdrawal of the needle from the specimen, and throughout this process, both the penetration load and the depth are meticulously recorded. The load scale (depicted in Figure 3, part 4) and the positioning of the presser on the penetration scale (Figure 3, part 3) are the critical elements in extracting this essential data. Subsequently, the cementation strength of the sample, denoted as NPR value, is computed using Equation (14):

$$NPR = F/D \tag{14}$$

In this equation, F represents penetration load in Newtons (N), while D signifies the penetration depth in millimeters (mm). The derived unit for NPR is N/mm. To further ascertain the UCS, the analysis continues with the application of Equation (15):

$$log\ (y) = 0.978\ log\ (x) + 2.621 \tag{15}$$

In this equation, x represents the penetration gradient, signifying the ratio between penetration load (N) and penetration depth (mm). The corresponding UCS value (y) is calculated through this relationship, as inferred from the UCS-NPR correlation chart. This meticulous testing procedure underlines the rigorous and standardized approach taken to estimate cementation strength, ensuring that the results provide valuable insights into the material's mechanical properties. The NPR is needle penetration resistance as a function of the penetration depth that can be used, in any direction, both in the field on out cropping rocks or loose blocks and in the laboratory on bore hole cores. The relationship between the UCS and NPR allows the radial strength to change of the stabilized soil (deterioration level) to be assessed.

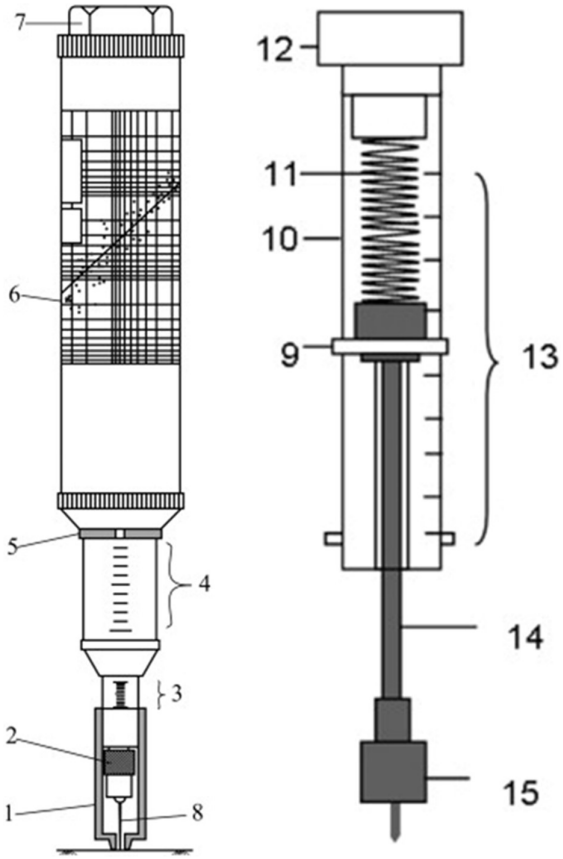

Figure 3. Schematic diagram of the Maruto penetrometers (Left) and inside illustration of the device (Right). (1) presser, (2) chuck, (3) penetration scale, (4) load scale, (5) load indication ring, (6) UCS–NPR correlation chart given by the manufacturer, (7) removable cap, (8) penetration needle, (9) indicator ring, (10) penetrometer tube, (11) spring, (12) end cap, (13) scale, (14) extension rod, and (15) needle block (after Ulusay, et al., 2015).

3 RESULTS AND DISCUSSIONS

3.1 Jute Fiber Reinforcement on the Process of $CaCO_3$ Precipitation

As depicted in Figure 5, the appearance of each specimen following 12 wetting-drying cycles in the retest reveals distinctive characteristics. The specimens that were incorporated with jute fiber displayed evolving shapes as the cycles progressed. In contrast, the specimens lacking jute fiber exhibited minimal deformation over the course of the wetting-drying cycles.

Figure 5 also shows the UCS of each test specimen before and after WD cycles, while figure 6 provides the mass loss each test specimen after each wetting-drying cycle test. Figures 5 and 6 enable the assessment of the impact of jute fiber reinforcement on the specimens' durability and strength. By comparing the UCS of specimen before WD cycles for 5 days (J-5 vs. NJ-5) or for 7 days (J-7 vs. NJ-7), it can be seen that the UCS with jute fiber has lower UCS that those without. The UCS of J-5 and J-7 are 0.11 MPa and 0.77 MPa respectively, whilst NJ-5 and NJ-7 are 0.82 MPa and 1.57 MPa respectively. After wetting-drying cycles with distilled water and artificial seawater, the 5 days treated specimen ruptured prior to UCS testing, i.e., UCS of 0 MPa. Whereas for the 7 days treated specimen, wetting-drying cycles with distilled water and artificial seawater reduced the UCS to 0.74 MPa (J-7-DW) and 0.35 MPa (J-7-AWS) respectively, a reduction of less than 5% and 55% respectively. For non-fiber-reinforced MICP specimen treated for 5 days and 7 days, they had a UCS of 0.82 MPa (NJ-5) and 1.57 MPa (NJ-7) respectively. After wetting-drying cycles with distilled water and artificial seawater, the UCS of 5 days treated specimen reduced to 0.67 MPa (NJ-5-AWS with 18% reduction) and 0.11 MPa (NJ-5-DW with 87% reduction) respectively; whereas for the 7 days treated specimen, the UCS reduced to 1.32 MPa (NJ-7-AWS with 16% reduction) and 1.41 MPa (NJ-7-DW 10% reduction) respectively. These findings indicate that the presence of jute fiber helps mitigate the reduction in UCS. However, it is noteworthy that, overall, the samples with jute fibers exhibit a lower UCS compared to those without. This observation likely explains why the mass loss was greater in specimens with jute fiber than in those without.

Figure 6 shows the variations in mass loss based on the soaking solution used and the presence of jute mixed in. Comparisons were made among specimens without jute fiber at 5 days curing time. NJ-5-AWS which was immersed in artificial seawater shows more significant mass loss (8.5%) compared to NJ-5-DW which was immersed in distilled water (4.5%). Secondly, comparisons were made among specimens with jute fiber. J-5-AWS which was immersed in artificial seawater shows less mass loss (10%) compared to J-5-DWS which was immersed in distilled water (22%). For 5 days curing time, the presence of jute fiber seems to improve the resistance of MICP-treated specimen against sea-water. However, it should be noted that MICP-treated specimen with jute fibers have a larger loss than without (10% and 22% vs. 8.5% and 4.5%).

The difference of soil specimen subjected to artificial sea water or distilled water become less apparent at 7 days curing time. For the specimens with jute fiber, J-7-AWS and J-7-DW have a mass loss difference of less than 1% (3% vs. 4%) with J-7-DW losing slightly more. On the other hand, specimens without jute fiber have similar loss at 2.5% for both NJ-7-AWS and NJ-7-DW. From the results, it seems that jute-reinforced MICP specimen perform better against seawater than distilled water. However, it should be noted that presence of jute resulted in increased mass loss than without jute. This result agrees with the observed UCS results, in which UCS of jute-reinforced specimens are lower than UCS of specimens without jute fibers.

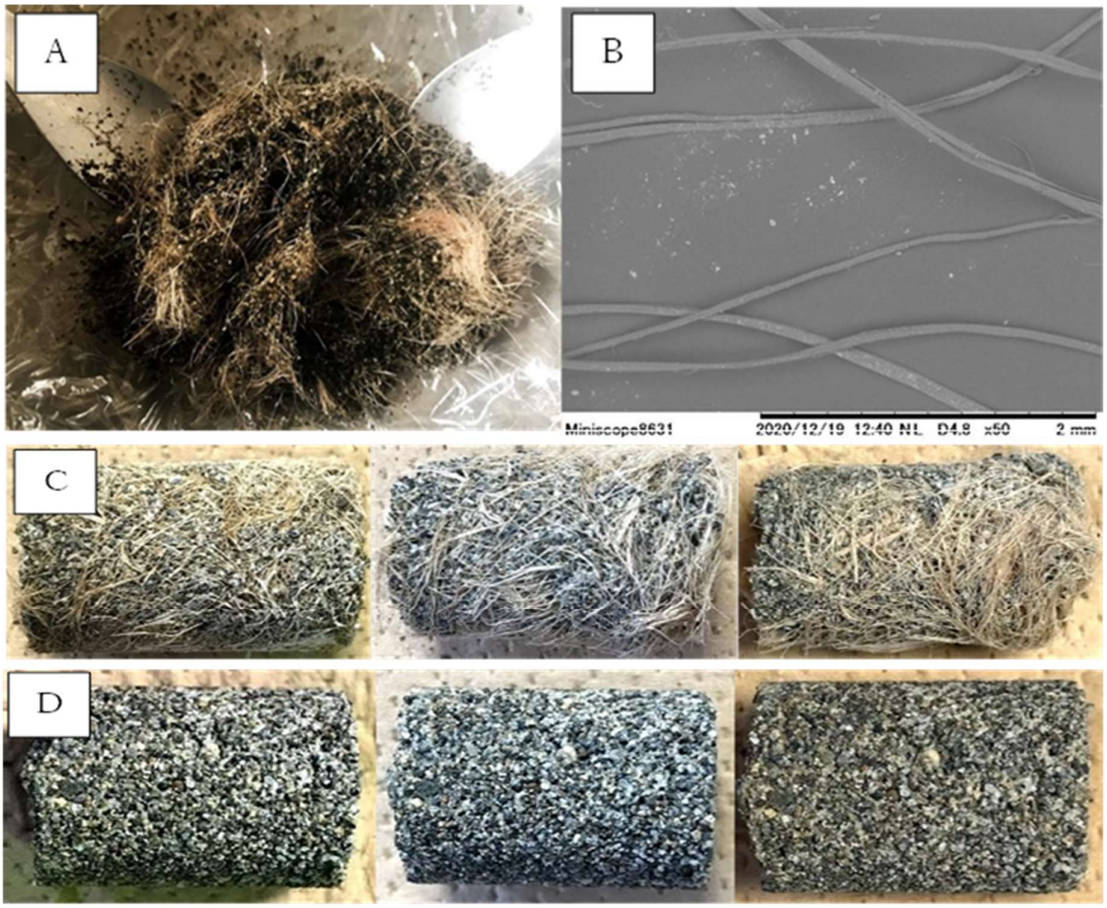

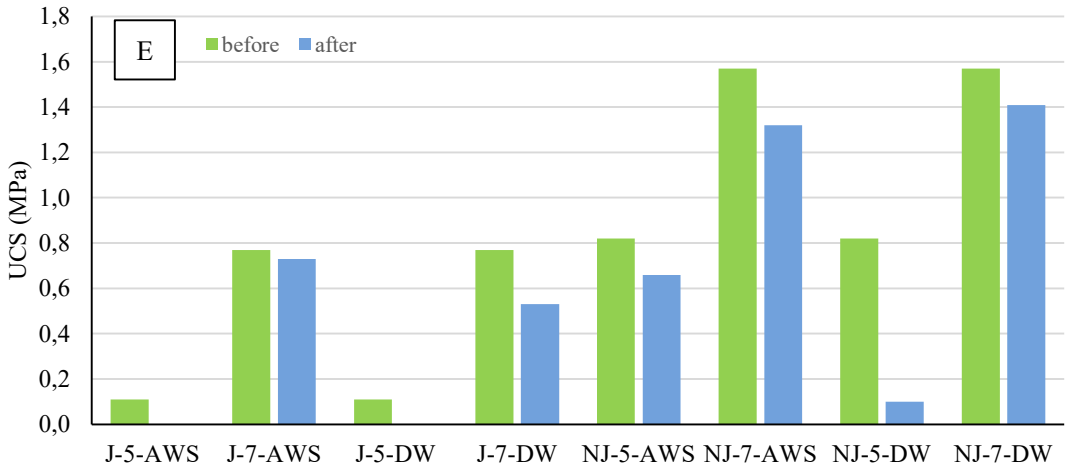

Figure 5. (A) Jute fibers added on the local Miyazaki silica sand, (B) SEM image of the jute fibers, (C) Aftertreatment of MICP mixed with jute reinforcement case, (D) MICP treatment without fibers, and (E, F) Estimates UCS Results of Needle Penetration Tested, Before and After WD Cycles.

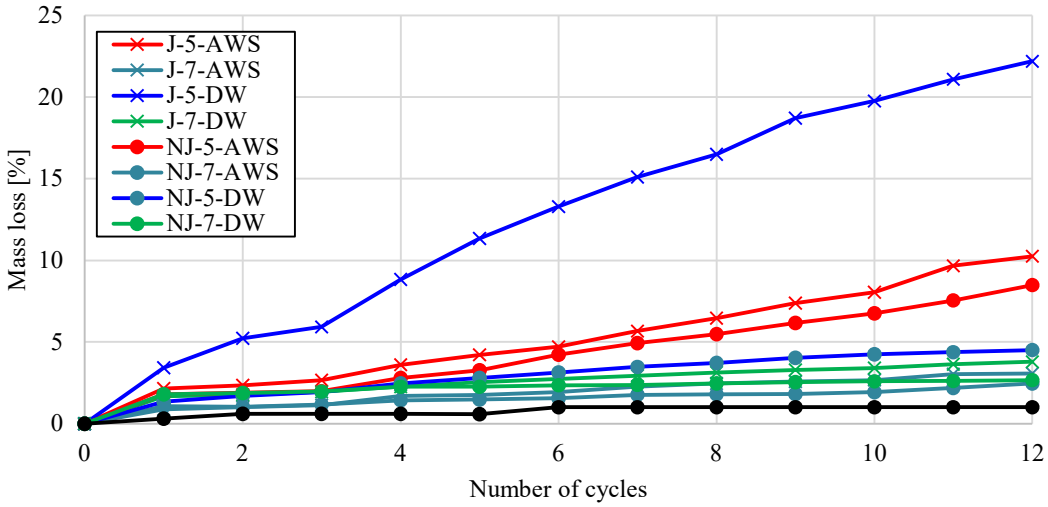

Figure 6. Average mass loss of the specimens subjected to WD cyclic treatments MICP treatment with and without jute reinforcement fibers

3.2 Behavior of Fiber-Reinforced Soil

The mass loss tended to become relatively stable (after several period of cycles), suggesting that the powdery deposits had been totally eroded. WD degradation mechanisms were proposed for geomaterials such as fracture energy reduction, capillary tension decrease, chemical and corrosive deterioration, frictional reduction, et cetera which cause the variation in thermal expansion coefficients and negative stress during the evaporation in this experiment samples (Zhao et al., 2017; Gowthaman et al., 2022; Daryono, et al., 2023). From the results, the reinforcement fibers can be done with randomly added material or arranged layering such as matt due to the mixing methods.

Broadly, fiber-reinforced soil can be categorized into two types based on their method of application:

(i) Oriented Distributed Fiber-reinforced Soil (ODFS)
(ii) Randomly Distributed Fiber-reinforced Soil (RDFS).

ODFS, a well-established soil reinforcement technique, offers a precise and versatile approach by allowing natural fibers to be introduced in controlled patterns, both vertically and horizontally. These patterns can be tailored to meet specific project requirements through various modifications such as weaving, binding, combining, or punching. This method uniformly increases the strength of the soil composite without introducing continuous planes of weakness. The inspiration for RDFS comes from the behavior of plant roots, which naturally enhance soil strength by contributing additional friction and interlocking mechanisms. The flexible nature of these fibers enables them to create a structural mesh that interlocks and binds the soil, thereby bolstering the structural integrity of the soil (Pollen, 2007; Ahmad et al., 2010). Figure 7 is shown the SEM images bonding between crystals of $CaCO_3$ from the MICP processes with jute fibers.

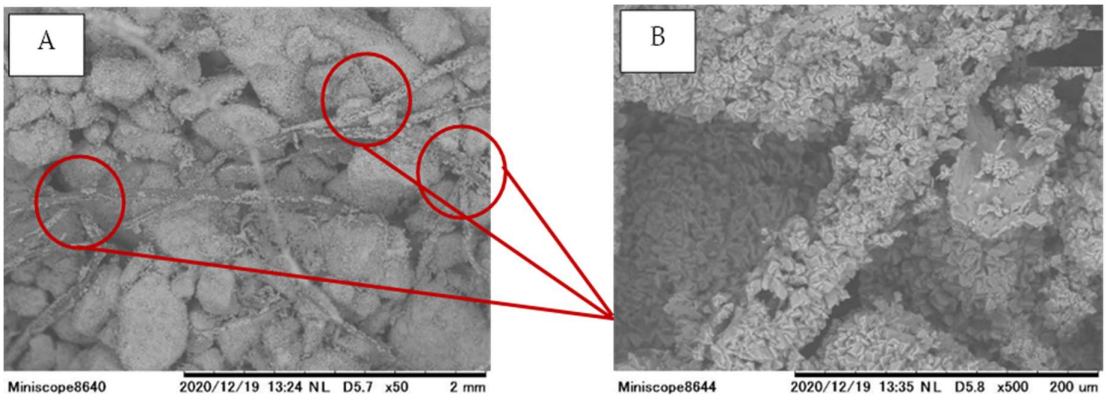

Figure 7. SEM images of bonding crystals CaCO3 with sands and jute fibers after treatment MICP with (A) bonding crystals in the fibers (×50 magnification) and (B) magnification with focus on only 1 fiber (×500 magnification).

4 CONCLUSION

Our understanding of fiber-matrix interaction, reinforcement mechanisms and performance characteristics is fairly advanced. Fiber reinforced is a promising material to be used in order to enhance for sustainable and long-lasting durability. The main findings obtained in this article are as follows.

(1) The mass reduction rate following 12 cycles of repetitive drying and wetting under the distilled water and also artificial sea water remained at 8.5% or less for the specimens that underwent the syringe solidification test for 7 days or 14 days based on the statistic of mass loss percentage. However, the material that added fiber experienced a drastic decrease in strength in this experiment where the material made was difficult to reduplicate results and testing the same sample with several analyses.

(2) The integrated fiber-reinforcement material mixed with MICP was proven to prevent the loss of mass during the wet-drying analysis caused by the fatigue damage due to the precipitation of the crystals and temperature shock in the materials. The longer the crystallization process with MICP takes, the stronger the material will be, where samples 5 days, 7 days, and 14 days show that the longer it takes, the more resistant it will be to weakening due to temperature factors.

(3) In future research, it will be essential to explore the reduction of the fiber content and carry out uniaxial compression tests employing larger-sized specimens for a more comprehensive analysis and also reproductivity of the analysis of the sample as standard for repeatability for long-term durable.

DISCLAIMER

The authors declare no conflict of interest.

AVAILABILITY OF DATA AND MATERIALS

The data underpinning the results and conclusions of this study can be obtained from the corresponding author1, upon reasonable request.

ACKNOWLEDGMENTS

The authors extend their heartfelt gratitude to all the individuals and entities involved in this collaborative research conducted between Hokkaido University and NITTOC Construction Ltd. While it is not feasible to acknowledge each contributor individually, their collective efforts and support have played a pivotal role in the successful completion of this study.

REFERENCES

Ahmad, F., Bateni, F. and Azmi, M., 2010. Performance evaluation of silty sand reinforced with fibers. *Geotextile and Geomembrane*, 28, pp. 93–99.

Akil, H.M., Cheng, L.W., Ishak, Z.A.M., Bakar, A.A.B. and Rahman, M.A.A., 2009. Water absorption study on pultruded jute fibre reinforced unsaturated polyester composites. *Composites Science and Technology*, 69, pp. 1942–1948.

Al-Swaidani, A., Hammoud, I. and Mezia, A. Effect of adding natural pozzolana on geotechnical properties of lime-stabilized clayey soil. *Journal of Rock Mechanics and Geotechnical Engineering*, 8(5), pp. 714–725.

Anbu, P., Kang, C.-H., Shin, Y.-J. and So, J.-S., 2016. Formations of calcium carbonate minerals by bacteria and its multiple applications. *Springerplus*, 5(1), pp. 1–26.

ASTM D559 (2003) Annual Book of ASTM Standards. ASTM, Philadelphia, PA., DOI: 10.1520/D0559-03.

Bera, A.K., Chandra, S.N., Ghosh, A., Ghosh, A., 2009. Unconfined compressive strength of fly ash reinforced with jute geotextiles. *Geotextile and Geomembrane*, 27, pp. 391–398.

Bundela, A.K., Lamoria, A., Singh, B., Tiwari, A., Sharma, A.K. and Dhemla, P., 2015. Identification of Weaker Subgrade Soil in Rajasthan and Increment of CBR by Jute Fiber as Additive. *Proceeding of Recent Development in Engineering, Science and Management*, 3, 109–113.

Burne, R.A. and Chen, Y.Y.M., 2000. Bacterial ureases in infectious diseases. *Microbes and Infection*, 2(5), pp. 533-542.

Chattopadhyay, B.C. and Chakravarty, S., 2009. Application of jute geotextiles as facilitator in drainage. *Geotextile and Geomembrane*, 27(2), 156–161.

Choi, S.G., Wang, K. and Chu, J., 2016. Properties of biocemented, fiber reinforced sand. *Construction and building materials*, 120, pp. 623-629.

Ciantia, M. O., Castellanza, R., Crosta, G. B. and Hueckel, T., 2015, Effects of mineral suspension and dissolution on strength and compressibility of soft carbonate rocks. *Engineering Geology*, 184, pp. 1–18.

Daryono, L.R., Nakashima, K., Kawasaki, S., Titisari, A.D. and Barianto, D.H., 2020a. Sediment characteristics of beachrock: A baseline investigation based on microbial induced carbonate precipitation at Krakal-Sadranan Beach, Yogyakarta, Indonesia. *Applied Sciences*, 10(2), p.520.

Daryono, L.R., Nakashima, K., Kawasaki, S., Suzuki, K, Suyanto, I. and Rahmadi, A., 2020b. Investigation of natural beachrock and physical–mechanical comparison with artificial beachrock induced by MICP as a protective measure against beach erosion at Yogyakarta, Indonesia. *Geosciences*, 10(4), p.143.

Daryono, L.R., Aoki, S., Kano, M., Miyanaga, M., Nakashima, K. and Kawasaki, S., 2024, January. Biomineralization Grouting for Beach Sand Cemented with MICP. *Journal of the Civil Engineering Forum*, 10(1), pp. 31-38.

Daryono, L.R., Aoki, S., Kano, M., Miyanaga, M., Nakashima, K. and Kawasaki, S., 2024. Biomineralization Grouting for Beach Sand Cemented with MICP. *Journal of the Civil Engineering Forum* pp. 31-38.

DeJong, J.T., Mortensen, B.M., Martinez, B.C. and Nelson, D.C., 2010. Bio-mediated soil improvement. *Ecological Engineering*, 36(2), pp.197-210.

Diambra, A., Ibraim, E., Wood, D.M. and Russell, A.R, 2010. Fibre reinforced sands: Experiments and modelling. *Geotextile and Geomembrane*, 28(3), pp. 238–250.

Ehrlich, H.L. and Newman, D.K., 2009. *Geomicrobiology of sulfur*. Boca Raton, Taylor & Francis, pp.439-489.

Fagone, M., Loccarini, F. and Ranocchiai, G., 2017. Strength evaluation of jute fabric for the reinforcement of rammed earth structures. *Composites Part B: Engineering*, 113, pp. 1–13.

Ghosha, S.K. Bhattacharyyab, R. and Mondal, M.M., 2017. Potential Applications of Open Weave Jute Geotextile (Soil Saver) in Meeting Geotechnical Difficulties. *Procedia Engineering*, 200, pp. 200–205.

Gosavi, M., Patil, K.A., Mittal, S. and Saran, S., 2004. Improvement of properties of black cotton soil subgrade through synthetic reinforcement. *Journal – Institution of Engineers India*, 84, pp. 257–262.

Gowthaman, S., Nakashima, K. and Kawasaki, S., 2018. A state-of-the-art review on soil reinforcement technology using natural plant fiber materials: Past findings, present trends and future directions. *Materials*, 11(4), p.553.

Gowthaman, S., Nakashima, K. and Kawasaki, S., 2022. Effect of wetting and drying cycles on the durability of bio-cemented soil of expressway slope. *International Journal of Environmental Science and Technology*, 19(4), pp.2309-2322.

Gowthaman, S., Nakashima, K. and Kawasaki, S., 2020. Freeze-thaw durability and shear responses of cemented slope soil treated by microbial induced carbonate precipitation. *Soils and Foundations*, 60(4), pp.840-855.

Gullu, H. and Khudir A., 2014, A. Effect of freeze-thaw cycles on unconfined compressive strength of fine-grained soil treated with jute fiber, steel fiber and lime. *Cold Regions. Science and Technology*, 106–107, pp. 55–65.

Imran, M.A., Gowthaman, S., Nakashima, K. and Kawasaki, S., 2020. The influence of the addition of plant-based natural fibers (Jute) on biocemented sand using MICP method. *Materials*, 13(18), p.4198.

Imran, M.A., Nakashima, K., Evelpidou, N. and Kawasaki, S., 2022. Durability improvement of biocemented sand by fiber-reinforced MICP for coastal erosion protection. *Materials*, 15(7), p.2389.

Kanchi, G., Neeraja, V. and Babu, S.G, 2014. Effect of anisotropy of fibers on the stress-strain response of fiber-reinforced soil. *International Journal of Geomechanics*, 15(1).

Kumari, D., Qian, X.Y., Pan, X., Achal, V., Li, Q. and Gadd, G.M., 2016. Microbially-induced carbonate precipitation for immobilization of toxic metals. *Advances in applied microbiology*, 94, pp. 79-108.

Kujawa, W., Olewnik-Kruszkowska, E. and Nowaczyk, J., 2021. Concrete strengthening by introducing polymer-based additives into the cement matrix—A mini review. *Materials*, 14(20), p.6071.

Liu, S., Wen, K., Armwood, C., Bu, C., Li, C., Amini, F. and Li, L., 2019. Enhancement of MICP-treated sandy soils against environmental deterioration. Journal of Materials in Civil Engineering, 31(12), p.04019294.

Michalowski, R.L. and Cermak, J. 2002. Strength anisotropy of fiber reinforced sand. *Computers and Geotechnics*, 29(4), pp. 279–299.

Muthukkumaran, K. and Shashank, B.S., 2016. Durability of microbially induced calcite precipitation (MICP) treated cohesionless soils. *Japanese Geotechnical Society Special Publication*, 2(56), pp. 1946-1949.

Pollen, N (2007). Temporal and spatial variability in root reinforcement of streambanks: Accounting for soil shear strength and moisture. *Catena*, 69(3), pp. 197–205.

Portugal, C.R.M., Fanyo, C., Machado, C.C., Meganck, R. & Jarvis, T., 2020. Microbiologically Induced Calcite Precipitation biocementation, green alternative for roads–is this the breakthrough? A critical review. *Journal of Cleaner Production*, 262, p.121372.

Ranganathan, S.R., 1994. Development and Potential of Jute Geotextiles. *Geotextile and Geomembr*ane, 13, pp. 421–433.

Saha, P.; Roy, D., Manna, S., Adhikari, B., Sen, R. and Roy, S., 2012. Durability of transesterified jute geotextiles. *Geotextile and Geomembr*ane, 35, 69–75.

Soupionis, G., Georgiou, P. and Zoumpoulakis, L., 2020. Polymer composite materials fiber-reinforced for the reinforcement/repair of concrete structures. *Polymers*, 12(9), p.2058.

Summerscales, J., Dissanayake, N.P.J., Virk, A.S. and Hall, W., 2010. A review of bast fibres and their composites. Part 1—Fibres as reinforcements. *Composites Part A: Applied Science and Manufacturing*, 41(10), pp. 1329–1335.

Tan, S.A.; Muhammad, N., and Karunaratne, G.P., 1994. Forming a Thin Sand Seam on a Clay Slurry with the Aid of a Jute Geotextile. *Geotextile and Geomembrane*, 13(11), 147–163.

Ulusay, R., Aydan, Ö., Erguler, Z.A., Ngan-Tillard, D.J., Seiki, T., Verwaal, W., Sasaki, Y. and Sato, A., 2015. ISRM suggested method for the needle penetration test. *The ISRM Suggested Methods for Rock Characterization, Testing and Monitoring: 2007-2014*, pp.143-155.

Wang, Y.X., Guo, P.P., Ren, W.X., Yuan, B.X., Yuan, H.P., Zhao, Y.L., Shan, S.B. & Cao, P., 2017. Laboratory Investigation on Strength Characteristics of Expansive Soil Treated with Jute Fiber Reinforcement. *International Journal of Geomechanics.* 17(11).

Zhao, Z., Yang, J., Zhang, D. and Peng, H., 2017. Effects of wetting and cyclic wetting–drying on tensile strength of sandstone with a low clay mineral content. *Rock Mechanics and Rock Engineering*, 50, pp. 485-491.

- This page is intentionally left blank -